J|A|C|S
ARTICLES
Published on Web 06/19/2004

Characterization, Supramolecular Assembly, and Nanostructures of Thiophene Dendrimers

Chuanjun Xia,[‡] Xiaowu Fan,[‡] Jason Locklin,[†] Rigoberto C. Advincula,*[,†,‡] Anthony Gies,[‡] and William Nonidez[‡]

Contribution from the Department of Chemistry, University of Houston, Houston, Texas 77204, and Department of Chemistry, The University of Alabama at Birmingham, Birmingham, Alabama 35394

Received March 18, 2004; E-mail: radvincula@uh.edu

Abstract: We report the synthesis and characterization of dendritic thiophene derivatives with their unique supramolecular assembly into 2-D crystals, nanowires, and nanoparticle aggregates. The structure and size of the dendrons and dendrimers have been confirmed with various techniques, such as NMR, SEC, and MALDI-TOF-MS. The mass values were consistent with the mass observed by MALDI-TOF-MS, whereas SEC measurements also gave useful information on the hydrodynamic volume of the individual dendrimers. The interesting electrooptical properties were highlighted by very broad absorption spectra and narrower fluorescence consistent with their electrochemical behavior. The self-organization of the dendrimers on the solid substrate is dependent on the nature of the substrate, preparation methods, and the molecule−molecule and molecule−substrate interactions. Thus, **14T-1** and **30T** both formed globular aggregates on mica surface, while **14T-1** also formed nanowires on graphite surface. On the other hand, the larger **30T** was observed to form 2-D crystalline structures. By varying the alkyl chain length attached to **14T-1**, we were also able to obtain 2-D crystals on graphite. This showed that the different symmetry of packing for **30T** and **14T-1** is also dependent on several factors, such as the molecular shape, size, and the presence of noncovalent intermolecular interactions. The results demonstrated the unique ability of thiophene dendrimers to form nanostructures on surfaces.

Introduction

Thiophene-related oligomers and polymers have remained one of the most well-studied π-conjugated systems in the past few decades because of their versatile chemistry as well as their applications in organic electronic devices.[1] The optical and electronic properties of thiophene derivatives can be easily tuned by varying the structure through the introduction of either different functional substituents or microstructures. For instance, the optical properties, packing behavior, and conductivity of regioregular polythiophenes differ significantly from those of regiorandom polythiophenes.[2] Although thiophene homopolymers, copolymers, and other related polymers and oligomers have been synthesized and investigated extensively,[3] not until recently have the all-thiophene dendritic derivatives been reported.[4]

As a recently developed and important class of polymers, dendrimers have received tremendous attention due to their unique architecture and potential applications in materials and life sciences.[5] Dendrimers bearing a rigid, conjugated backbone have also been designed.[6] These dendrimers, so-called conjugated dendrimers, were first studied by the Moore group. They designed a series of phenylacetylene dendrimers together with their perylene-substituted derivatives with nanoscale dimension and studied their energetic absorption and energy-funneling

[†] University of Houston.

[‡] The University of Alabama at Birmingham.

(1) (a) *Electronic Materials: The Oligomer Approach*; Mullen, K., Wegner, G., Eds.; Wiley-VCH: New York, 1998. (b) *Handbook of Oligo- and Polythiophenes*; Fichou, D., Ed.; Wiley-VCH: New York, 1999. (c) Fichou, D. *J. Mater. Chem.* **2000**, *10*, 571−588.

(2) McCullough, R. D. *Adv. Mater.* **1998**, *10*, 93−116.

(3) (a) Fuhrmann, G.; Kromer, J.; Bauerle, P. *Synth. Met.* **2001**, *119*, 125−126. (b) Kromer, J.; Rios-Carreras, I.; Fuhrmann, G.; Musch, C.; Wunderlin, M.; Debaerdemaeker, T.; Mena-Osteritz, E.; Bauerle, P. *Angew. Chem.* **2000**, *39*, 3469−3481. (c) Marsella, M. J.; Yoon, K.; Tham, F. S. *Org. Lett.* **2001**, *3*, 2129−2131. (d) Swager, T. M.; Marsella, M. J. *J. Am. Chem. Soc.* **1993**, *115*, 12214−12215. (e) Yu, W.-L.; Meng, H.; Pei, J.; Huang, W. *J. Am. Chem. Soc.* **1998**, *120*, 11808−11809. (f) Malenfant, P. R. L.; Groenendaal, L.; Frechet, J. M. J. *J. Am. Chem. Soc.* **1998**, *120*, 10990−10991. (g) Hempenius, M. A.; Langeveld-Voss, B. M. W.; Haare, J. A. E. H. v.; Janssen, R. A. J.; Sheiko, S. S.; Spatz, J. P.; Moller, M.; Meijer, E. W. *J. Am. Chem. Soc.* **1998**, *120*, 2798−2804.

(4) Xia, C.; Fan, X.; Locklin, J.; Advincula, R. C. *Org. Lett.* **2002**, *4*, 2067−2070.

(5) For books and reviews about dendrimers, see: (a) Bosman, A. W.; Janssen, H. M.; Meijer, E. W. *Chem. Rev.* **1999**, *99*, 1665−1688. (b) Fischer, M.; Vogtle, F. *Angew. Chem., Int. Ed.* **1999**, *38*, 884−905. (c) Grayson, S. M.; Frechet, J. M. J. *Chem. Rev.* **2001**, *101*, 3819−3868. (d) Zimmerman, S. C. *Chem. Rev.* **1997**, *97*, 1681−1712. (e) *Dendrimers*; Vogtle, F., Ed.; Topics in Current Chemistry, Vol. 197; Springer: Berlin, 1998. (f) *Dendrimers II: Architecture, Nanostructure and Supramolecular Chemistry*; Vogtle, F., Ed.; Topics in Current Chemistry, Vol. 210; Springer: Berlin, 2000. (g) *Dendrimers III: Design, Dimension, Function*; Vogtle, F., Ed.; Topics in Current Chemistry, Vol. 212; Springer: Berlin, 2001. (h) *Dendrimers IV: Metal Coordination, Self-Assembly, Catalysis*; Vogtle, F., Schalley, C. A., Eds.; Topics in Current Chemistry, Vol. 217; Springer: Berlin, 2001.

(6) (a) Moore, J. S. *Acc. Chem. Res.* **1997**, *30*, 402−413. (b) Gong, L.; Hu, Q.; Pu, L. *J. Org. Chem.* **2001**, *66*, 2358−2367. (c) Deb, S. K.; Maddux, T. M.; Yu, L. *J. Am. Chem. Soc.* **1997**, *119*, 9079−9080. (d) Meier, H.; Lehmann, M. *Angew. Chem., Int. Ed.* **1998**, *37*, 643−645. (e) Lupton, J. M.; Samuel, I. D. W.; Beavington, R.; Burn, P. L.; Bassler, H. *Adv. Mater.* **2001**, *13*, 258−261. (f) Berresheim, A. J.; Muller, M.; Mullen, K. *Chem. Rev.* **1999**, *99*, 1747−1786.

characteristics.[7] The interests in these kinds of shape-persistent conjugated dendrimers have increased rapidly in recent years. Conjugated dendrimers with other backbones have also been synthesized. Müllen et al.[8] recently demonstrated the synthesis of phenylene dendrimers using a convergent method starting with the deprotection of 4,4′-di(triisopropyl)-ethynylbenzil, a tetraphenylcyclopentadienone precursor through a [4+2]-cycloaddition reaction. This approach is useful for the rapid synthesis of dendritic polyphenylene structures of greater size and with fewer growth imperfections.

When compared to their linear analogues, conjugated dendrimers have a number of potential advantages in terms of applications in optoelectronics. Their shape persistency allows them to maintain structure in a solution-processable form, which can therefore minimize the π-stacking, and increase quantum efficiency. In addition, an internal local electric field may be created during the charge transfer to the core of the dendrimer, which can capture opposite charges. This strategy has been adopted for designing novel materials for organic light-emitting diode (OLED) applications.[9] However, the study of dendrimer aggregation behavior in the solid state, or in ultrathin films, seems to be more intriguing because of their monodisperse and periodic structures. Supramolecular structures do form for some of these dendrimers. For example, the phenylene dendrimers can self-assemble into nanowires and other supramolecular structures as a result of $\pi-\pi$-stacking interactions.[10]

We have reported the design and synthesis of a novel class of thiophene dendrons and dendrimers in a previous paper.[4] This design introduces a novel architecture for thiophene derivatives, enriching thiophene chemistry, and providing greater opportunity to study their properties, assembly, and applications in organic and molecular electronics. In the present paper, we wish to report our investigations on the structural characterization, size information, optical properties, and supramolecular assembly on different solid substrates of these materials. The nanostructures observed from these materials exhibit both short-range and long-range ordering primarily through the influence of $\pi-\pi$-stacking properties of the thiophene rings and the van der Waals forces derived from the packing of the alkyl chains.

Results and Discussion

Synthesis. The structures of the dendrons and dendrimers **3T**, **7T**, **15T**, **6T**, and **14T-1** are shown in Chart 1. The synthesis of these compounds has been described previously.[4] The starting materials for the syntheses of **14T-2** and **30T** are shown in Scheme 1. As shown in Scheme 1, the lithiation of 2,3-dibromothiophene with LDA gave 2-lithium-3,5-dibromothiophene rather than 3-lithium-4,5-dibromothiophene (as previously assigned) due to the "base-catalyzed halogen dance" known to occur in thiophenes.[11] The coupling product was thus 3,5,3′,5′-tetrabromo-[2,2′]bithiophenyl. The structure has been confirmed by comparison with a model compound that was synthesized through tetrabromination of bithiophene, which was known to give 3,5,3′,5′-tetrabromo-[2,2′]bithiophenyl.[12] The exact structures of the dendrimers **14T-2** and **30T** are thus shown in Scheme 2.

Chart 1. Structures of the Other Thiophene Dendrons and Dendrimers (the Names Were Given after the Number of the Repeating Units)

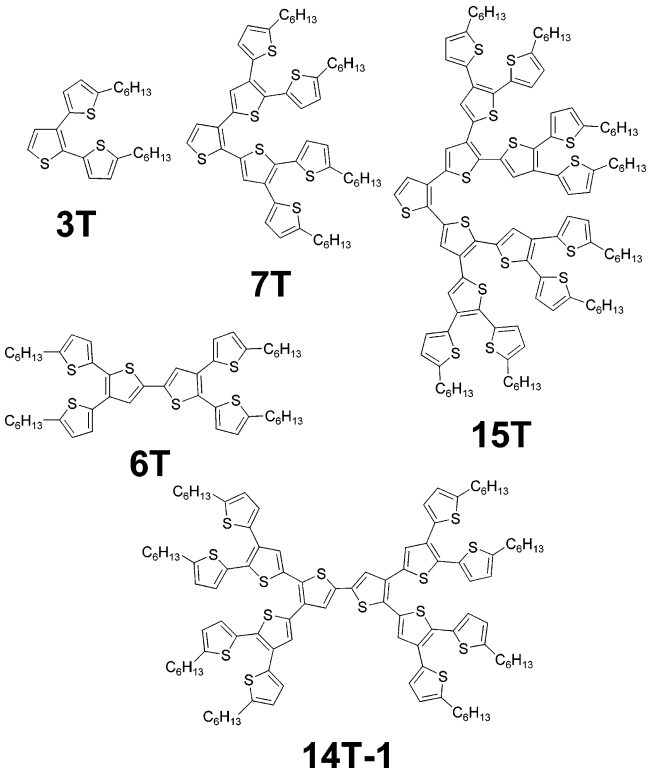

Scheme 1. Synthesis Route Using a Combination of Cross-Coupling Reactions To Form the Monomers and Tetrafunctional Core Group

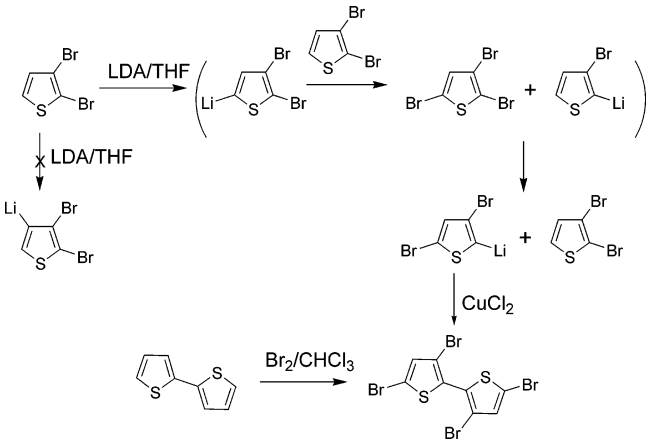

NMR Characterization. All of the thiophene dendrons and dendrimers shown in Chart 1 are highly soluble in common solvents such as chloroform, THF, and even hexane. Polar solvents such as DMF and DMSO cannot dissolve compounds

(7) Devadoss, C.; Bharathi, P.; Moore, J. S. *J. Am. Chem. Soc.* **1996**, *118*, 9635−9644.
(8) (a) Morgenroth, F.; Kubel, C.; Mullen, K. *J. Mater. Chem.* **1997**, *7*, 1207−1211. (b) Morgenroth, F.; Reuther, E.; Mullen, K. *Angew. Chem., Int. Ed. Engl.* **1997**, *36*, 631−634.
(9) (a) Wang, P. W.; Liu, Y. J.; Devadoss, C.; Bharathi, P.; Moore, J. S. *Adv. Mater.* **1996**, *8*, 237−241. (b) Bettenhausen, J.; Strohriegl, P.; Brutting, W.; Tokuhisa, H.; Tsutsui, T. *J. Appl. Phys.* **1997**, *82*, 4957−4961. (c) Glebeler, C.; Antoniadis, H.; Bradley, D. D. C.; Shirota, Y. *Appl. Phys. Lett.* **1998**, *72*, 2448−2450. (d) Halim, M.; Samuel, I. D. W.; Pillow, J. N. D.; Monkman, A. P.; Burn, P. L. *Synth. Met.* **1999**, *102*, 1571−1574.
(10) (a) Liu, D.; Zhang, H.; Grim, P. C. M.; De Feyter, S.; Wiesler, U.-M.; Berresheim, A. J.; Mullen, K.; De Schryver, F. C. *Langmuir* **2002**, *18*, 2385−2391. (b) Loi, S.; Butt, H.-J.; Hampel, C.; Bauer, R.; Wiesler, U.-M.; Mullen, K. *Langmuir* **2002**, *18*, 2398−2405. (c) Loi, S.; Wiesler, U.-M.; Butt, H.-J.; Mullen, K. *Macromolecules* **2001**, *34*, 3661−3671.
(11) Frohlich, H.; Kalt, W. *J. Org. Chem.* **1990**, *55*, 2993−2995.
(12) Yu, W.-L.; Meng, H.; Pei, J.; Huang, W.; Li, Y.; Heeger, A. J. *Macromolecules* **1998**, *31*, 4838−4844.

Scheme 2. A Convergent Synthesis Route for the **14T-2** and **30T** Dendrimers by Simply Tethering the Dendrons to the Tetrafunctional Core

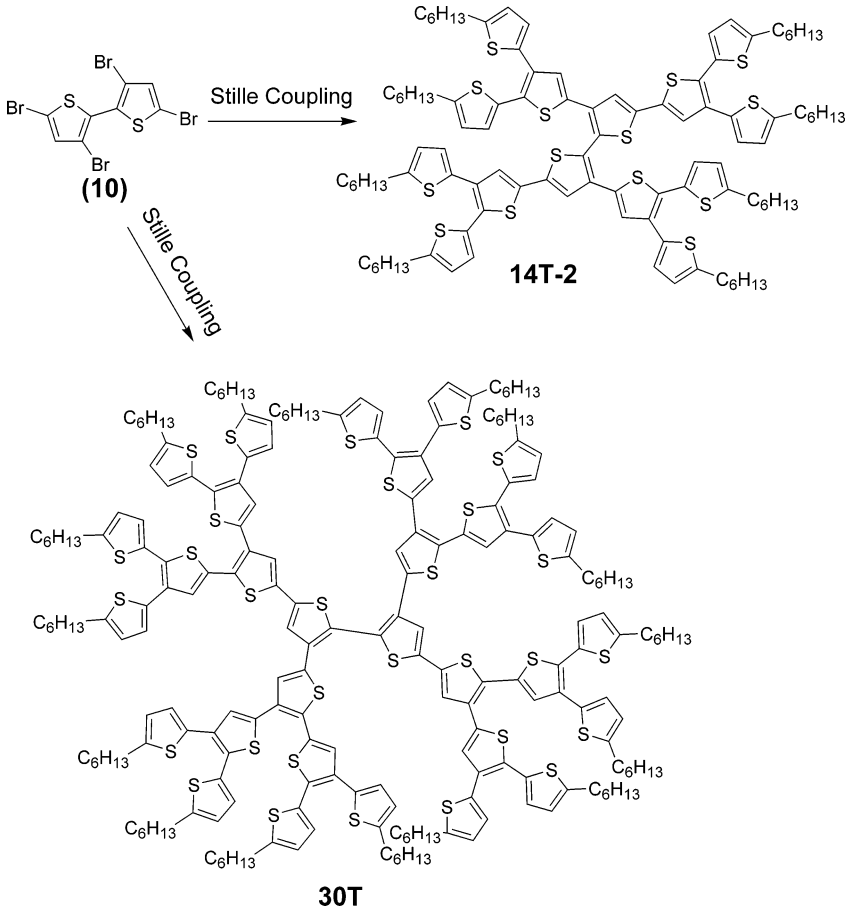

bigger than **7T** at room temperature. NMR spectra of those compounds larger than **7T** differ, in both peak position and splitting pattern, when running in different solvents, such as chloroform-*d*, THF-d_8, and methylene chloride-d_2. This phenomenon indicates different associations of the molecules in different solvents.[13] Figure 1 shows the aromatic region of the ^{1}H NMR spectra of **14T-1**, **14T-2**, and **30T** in THF-d_8 at 290 K. The interior protons on the thiophene ring show singlets downfield, and the exterior protons show doublets upfield. The doublets of the protons from the outermost shell of the thiophene rings are located below 7.00 ppm. The resonance shifts downfield on moving to the inner thiophene units. The protons on the central thiophene ring have the most downfield resonance peaks. The resonance of the protons on the thiophene ring in the aromatic region is also temperature dependent. Temperature-controlled experiments were performed for **14T-1**, **14T-2**, and **30T** in THF-d_8. Upon cooling, the resonances of those singlet protons were significantly shifted downfield. Only small shifts were observed for the external protons. This would indicate that the rigidity of the thiophene units in the dendrimer is different. This observation indicates that less hindered rotation is present in the external thiophene units of the dendrimer than those units in the core. The chemical shifts of the most downfield singlet proton and the most upfield doublet proton in the aromatic region against temperature are plotted for the dendrimers in Figure 2.

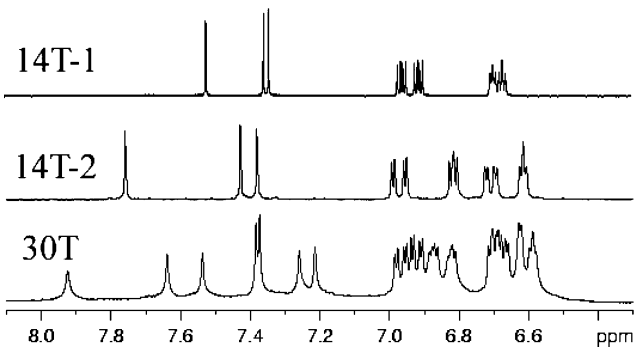

Figure 1. ^{1}H NMR spectra of **14T-1**, **14T-2**, and **30T** in THF-d_8 at 290 K. Only the aromatic region is shown.

MALDI-TOF-MS. Figure 3 displays the MALDI-TOF-MS spectra of **14T-1**, **14T-2**, and **30T**. The insets show the expanded spectra. As expected, the peak masses from the mass spectra are well correlated with the proposed structures. The spectra indicate the monodispersity of the dendrimers. High resolution could be obtained through a reflectron mode. Mass values from different isotopes can be easily distinguished. For **30T**, a few small peaks appeared at the mass region between 3500 and 3800. These peaks could be due to the fragmentation of the dendrimer or impurities. The possibility of these peaks originating from impurities can be ruled out by examining the synthesis procedure.[4] **30T** was synthesized from a coupling method, in which four arms were connected to the central core. Therefore, masses with fewer arms should be observed from the mass

(13) Shetty, A. S.; Zhang, J.; Moore, J. S. *J. Am. Chem. Soc.* **1996**, *118*, 1019−1027.

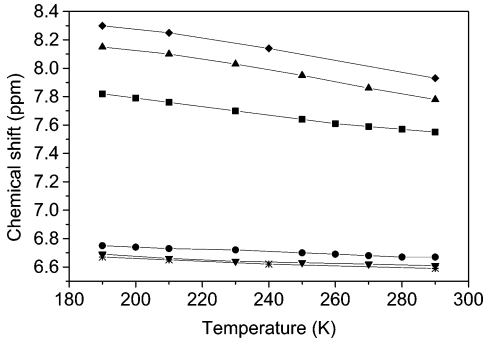

Figure 2. The chemical shifts of the most downfield singlet and the most upfield doublet protons on the thiophene rings under different temperatures in THF-d_8. **14T-1**, ■ ●; **14T-2**, ▲ ▼; **30T**, ◆*.

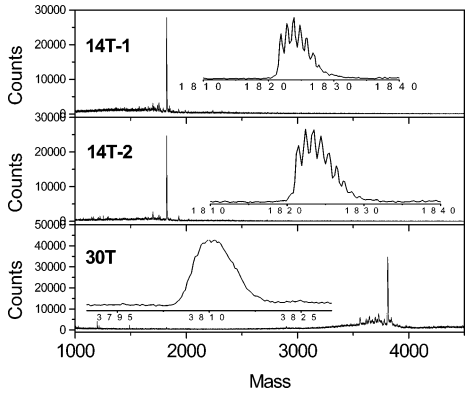

Figure 3. MALDI-TOF-MS spectra of **14T-1**, **14T-2**, and **30T**. The insets show the expanded spectra.

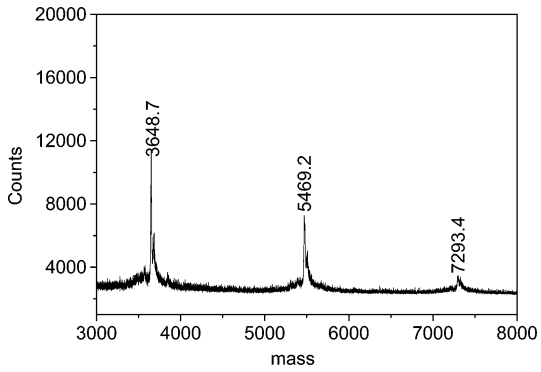

Figure 4. MALDI-TOF-MS spectrum of **14T-1** collected with the linear mode.

spectrum if the coupling reaction was not complete. However, those peaks did not appear in the spectrum considering that the mass of a single arm is ~912 Da.

When operating in the linear mode, which has better sensitivity but lower resolution, the aggregates of the dendrimers started to appear in the spectra. Figure 4 depicts the aggregation of **14T-1**. Besides the major peak at the molecular mass (1923 Da), peaks at 3648.7, 5469.2, and 7293.4 were also observed with much lower intensities, which correspond to the dimer, trimer, and tetramer aggregates, respectively. **14T-2** only showed weak aggregation peaks under the same experimental conditions. Higher laser power was required for **30T** due to its larger size. The aggregation of shape-persistent macrocyclic amphiphilic poly(phenyl acetylene)s was previously investigated by MALDI-TOF-MS by Hoger et al.[14] They attributed the origin of aggregate formation to either the $\pi-\pi$-stacking of aromatic units

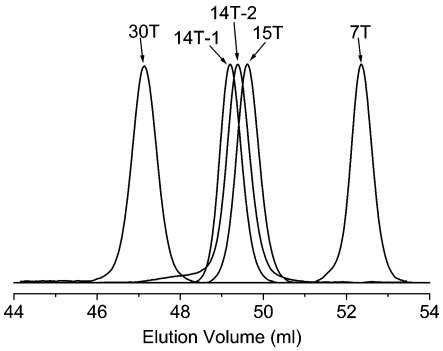

Figure 5. SEC traces of **7T**, **14T-1**, **14T-2**, **15T**, and **30T** using THF as the solvent.

Table 1. Calculated Mass, Mass from MALDI-TOF-MS, Number-Average Molecular Weight from SEC, and Polydispersity of the Compounds

	calculated mass	MALDI	M_n	DPI
7T	913.5		989	1.01
14T-1	1823.6	1824.0	1955	1.01
14T-2	1823.6	1823.6	1903	1.01
15T	1905.6	1905.3	1791	1.01
30T	3809.2	3809.5	3202	1.01

of flat macrocycles or the aggregation via hydrogen bonding between the polar phenoxy groups of the ring. In our current study, the π-interaction between the aromatic systems seems to be the only origin of aggregation. The planarity of the macromolecule plays an important role in the aggregation. The more planar the molecule is, the stronger are the intermolecular forces that occur. The less aggregates formed for **14T-2** and **30T** indicated less planarity for these molecules. Considering the structures of the three dendrimers, more steric hindrance was caused by the adjacent thiophene units in **14T-2** and **30T** than in **14T-1**, thus decreasing the planarity of the molecules and π-conjugation. This was also consistent with their absorption spectra. The aggregates formed either during the MALDI sample preparation or in the gas phase (right after the desorption and ionization process), or both.

SEC Studies. Although deviations are normally observed when characterizing these rigid linear or dendritic polymers by size exclusion chromatography using polystyrene as the calibration standard, useful information about the molecules may still be obtained. Figure 5 shows the SEC traces of the thiophene dendrons and dendrimers. Interestingly, the hydrodynamic volume of these molecules is directly related to their size and structure. For instance, **14T-1** has a lower elution volume than **14T-2** despite the fact that they have the same molecular weight. Again, **14T-2** exhibits a more condensed structure than **14T-1**. The wedge-shaped molecule, **15T**, has even higher elution volume than **14T-1** and **14T-2,** yet it has one more thiophene unit. This behavior can also be explained by the size of the molecule. It is obvious that the 2,3-disubstitution of the central thiophene unit in **15T** is more crowded than the α,α or α,β coupling in **14T-1** and **14T-2**. Table 1 summarizes the results from MALDI-TOF-MS and SEC. The masses from MALDI-TOF-MS are very consistent with the actual value calculated from the molecular structures. On the other hand, the number-

(14) Hoger, S.; Spickermann, J.; Morrison, D. L.; Dziezok, P.; Rader, H. J. *Macromolecules* **1997**, *30*, 3110−3111.

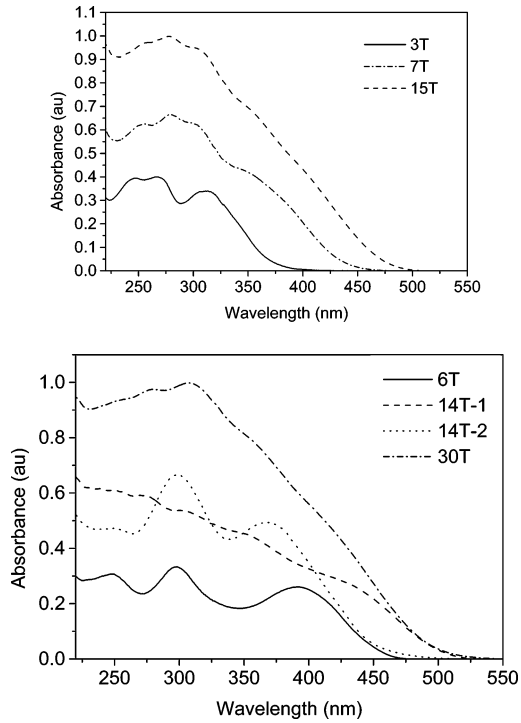

Figure 6. Absorption spectra of the dendrons and dendrimers in THF.

average molecular weights from SEC somehow deviate from their true value. All of the SEC traces showed monodispersity for all of the dendrons and dendrimers examined. Although polydispersity from SEC does not often give precise information when measuring big dendritic molecules,[15] the polydispersity results shown here are quite valid if one considers the rather small sizes and high resolution of the columns. A slight structure variation will cause a detectable difference in the SEC traces. When carefully examining the values from SEC measurements, one may notice that the number-average molecular weights for **6T**, **14T-1**, and **14T-2** are higher than their true value, but lower for **15T** and **30T**. There is a more significant deviation for **30T**. SEC tends to overestimate the molecular weights when it is used to study the linear rigid conjugated polymers using polystyrene standards.[16] On the other hand, it often underestimates the molecular weights when measuring dendritic systems because of their condensed structures. For these thiophene compounds, a transition occurs when going from low-generation to high-generation dendrimers.

Spectroscopic Properties. These dendritic molecules show spectroscopic properties that are drastically different from those of linear thiophene oligomers and polymers (Figure 6). As mentioned earlier, the connection between each thiophene unit includes α,α and α,β linkages, where α,α linkage provides the best π-electron conjugation, and the others may disrupt it. For the monodendrons, as the generation number increases, the absorption spectra shift to longer wavelength, with the absorption onset at 372, 440, and 473 for **3T**, **7T**, and **15T**, respectively. The absorption spectrum of **3T** shows three discernible peaks at 310, 268, and 247 nm. The peak at 310 nm shows a typical vibrationless vibronic (0−0) transition, and the other two higher-energy absorption peaks are assigned to the vibronic 0−1 and 0−2 transitions. The longest absorption maximum is only about 10 nm red-shifted to that of 2,2′-bithiophene, and this wavelength is about 60 nm shorter than that of α-terthiophene, which is the linear analogue with all α,α linkages between each thiophene unit.

For **7T** and **15T**, no discernible peaks are observable in the long wavelength region, and only a featureless tail appears. Interestingly, both have three peaks located at around the same position as **3T**. Previous investigations on the absorption spectra of a series of symmetrical polyphenylene acetylene dendrimers have shown that localized electronic excitations can be present, showing peaks at energies that are characteristic of excitations localized on different conjugation lengths.[17] The observations with the thiophene dendrons clearly show the presence of excitations localized on different conjugation lengths.

Figure 6 shows the absorption spectra of **6T**, **14T-1**, **14T-2**, and **30T**. All of them show broad absorption, but with different signatures. **6T** has three peaks at 392, 298, and 248 nm, originating from the $\pi-\pi^*$ transitions. The lowest excitation of **6T** is almost identical to α-quaterthiophene. This result indicates that the α,α-linked thiophene segment provides the longest conjugation length. On the other hand, the different linkage of the central thiophene units for **14T-2** and **30T** does interrupt the π-conjugation. The absorption onset of **14T-2** and **30T** only shifts to longer wavelength by 14 and 24 nm, respectively, as compared to **7T** and **15T**. In addition, the localized excitation is more evident for **14T-2** than that of **14T-1** from the spectra. Besides the longer absorption onset (501 nm), **14T-1** has a featureless broad absorption from 220 to 500 nm.

The fluorescence spectra of the dendritic molecules in THF are shown in Figure 7. The fluorescence of the thiophene dendrons shifts to longer wavelength as the generation increases. This result is similar to a series of unsymmetrical phenylene acetylene dendrimers recently reported by Peng et al.,[18] which is certainly reasonable because of the unsymmetrical nature of the thiophene dendrimer. The shape of the fluorescence spectra is insensitive to the excitation wavelength in a wide range. The emission in this case originates from the longest conjugated segment in the molecule. The results are summarized in Table 2. The location and shape of the fluorescence spectra indicate an intramolecular energy transfer from the higher band-gap branches to the lowest one. It is interesting that **14T-2** exhibits an unusually broad and long wavelength emission as compared to **14T-1** despite having the same mass. The intramolecular energy transfer and the photophysics of this system need further investigation.

Electrochemistry. The electrochemical properties of **14T-1**, **14T-2**, and **30T** were investigated by cyclic voltammetry. Figure 8 shows the cyclic voltammetric response of **14T-1**, **14T-2**, and **30T**. The redox behavior of these compounds is markedly different from one another due to their different structures. For **14T-1**, two peaks at 0.45 and 0.81 V were observed during the anodic scans upon oxidation. The first wave is reversible, with a peak at 0.30 V during the cathodic scan, and the second one is ill-defined, which indicates a fast follow-up reaction after the second oxidation. Upon reduction, two pairs with a main

(15) Bu, L.; Nonidez, W. K.; Mays, J. W.; Tan, N. B. *Macromolecules* **2000**, *33*, 4445−4452.
(16) Liu, J.; Loewe, R. S.; McCullough, R. D. *Macromolecules* **1999**, *32*, 5777−5785.
(17) Kopelman, R.; Shortreed, M. R.; Shi, Z. Y.; Tan, W.; Xu, Z.; Moore, J. S. *Phys. Rev. Lett.* **1997**, *78*, 1239−1242.
(18) Peng, Z.; Pan, Y.; Xu, B.; Zhang, J. *J. Am. Chem. Soc.* **2000**, *122*, 6619−6623.

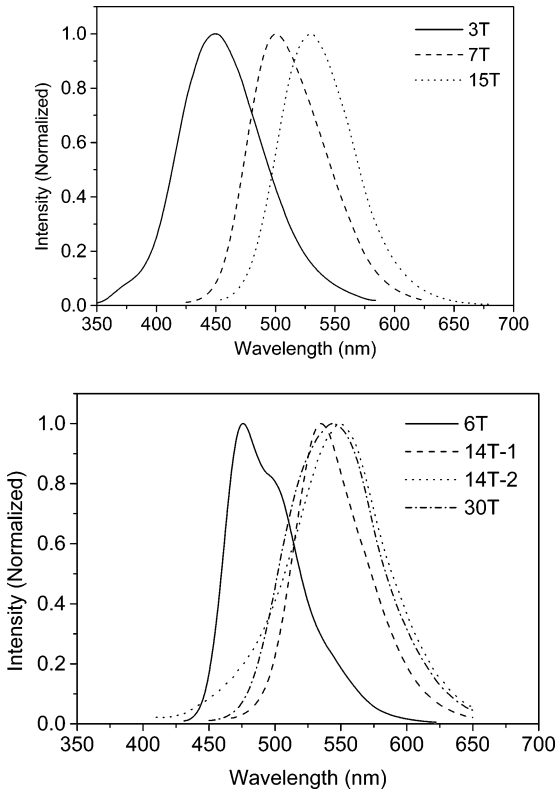

Figure 7. Fluorescence spectra of the dendrons and dendrimers in THF.

Table 2. Absorption Onset, Band Gap Calculated from the Absorption Onset, Photoluminescence Maxima, and the Molar Extinction Coefficient for the Dendritic Molecules

compound	absorption onset (nm)	band gap (eV)	PL maximum (nm)	ϵ_{max}[a] (M^{-1} cm^{-1})
3T	372	3.33	449	9700
6T	458	2.71	476	28 500
7T	440	2.82	500	25 800
14T-1	501	2.48	534	49 200
14T-2	454	2.73	549	
15T	473	2.62	529	56 400
30T	497	2.50	543	

[a] The extinction coefficient was determined at the absorption maxima in methylene chloride.

peak at −2.47/−2.27 V and a small shoulder at −2.58/−2.51 V were observed. On the other hand, the cyclic voltammogram of **14T-2** exhibited reversible waves in both the oxidation and the reduction parts. Two reversible waves can be clearly seen at 0.47 and 0.68 V upon oxidation, followed by two peaks at 0.38 and 0.60 V during the cathodic scan. The reduction peaks are located at −2.43/−2.33 V. **30T** only shows an ill-defined and mainly irreversible CV process. Three oxidation peaks at 0.47, 0.64, and 0.89 V are barely distinguished. Two peaks at −2.38 and −2.61 V can also be seen upon reduction. Note that the size of **30T** is significantly larger than those of **14T-1** and **14T-2**. It was previously found that the redox behavior of dendritic porphyrins is greatly influenced by dendrimeric branching around the porphyrin core.[19] The CV becomes ill-defined and irreversible when the surrounding dendrimeric branching is significantly large. Although the redox processes are not comparable, the large size of the molecule, which results

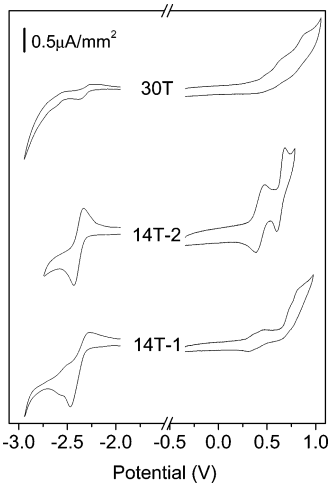

Figure 8. Cyclic voltammagram of **14T-1**, **14T-2**, and **30T**. The Ag/Ag^+ electrode was used as the reference electrode and was calibrated with ferrocene/ferrocium coupling. The shown potential is against Fc/Fc^+. Tetrabutylammonium hexafluorophosphate was used as supporting electrolyte (0.1 M). The oxidation was performed in anhydrous methylene chloride, and the reduction was performed in dry THF under argon atmosphere.

in a small diffusion coefficient, may play the same role in this case. The band gaps calculated for **14T-1**, **14T-2**, and **30T** on the basis of the oxidation and reduction onsets are 2.46, 2.72, and 2.51 eV, respectively, and are consistent with those calculated from the absorption spectra onset. Carefully examining the structures of these three compounds should give us more insight into their electrochemical properties. Considering the case of **14T-1** and **14T-2**, the only difference lies in the linkage of the innermost bithiophene unit: a 4,5,4′5′ linkage for **14T-1** and a 3,5,3′5′ linkage for **14T-2**. As has been studied, the oxidation potential decreases as the conjugation length increases from short OTs to PTs, although the oxidation wave becomes extremely broad.[18] In this case, **14T-1** apparently has a longer conjugation length than **14T-2**, so that it is oxidized at about 80 mV lower than **14T-2**.

Supramolecular Assembly. Linear thiophene derivatives are well known to form supramolecular structures on solid substrates. Depending on the energy difference between the molecule−substrate and the molecule−molecule, either 2-D crystals or nanoribbon structures can be formed.[1,2] As shown by Meijer et al.,[20] strong $\pi-\pi$ interactions between each sexithiophene unit governed the supramolecular assembly on graphite or silicon substrate and formed ribbonlike structures. When the molecule−substrate interaction is strong, a sensibly packed 2-D crystal structure can be observed, as shown by Bäuerle et al.,[21] where the strong hydrophobic interaction between the graphite and the long alkyl chain greatly facilitated the 2-D packing of the oligothiophenes.

We investigated the self-organization of **14T-1** and **30T** on two types of substrates: mica and highly ordered pyrolytic graphite (HOPG). The films were prepared through solvent casting from solutions with different concentrations. The solvent was allowed to evaporate very slowly in a nearly closed glass

(19) Dandliker, P.; Diederich, F.; Gross, M.; Knobler, C.; Louati, A.; Sanford, E. *Angew. Chem., Int. Ed. Engl.* **1994**, *33*, 1739−1742.

(20) Schenning, A. P. H. J.; Kilbinger, A. F. M.; Biscarini, F.; Cavallini, M.; Cooper, H. J.; Derrick, P. J.; Feast, W. J.; Lazzaroni, R.; Leclere, Ph.; McDonell, L. A.; Meijer, E. W.; Meskers, S. C. J. *J. Am. Chem. Soc.* **2002**, *124*, 1269−1275.

(21) Bauerle, P.; Fischer, T.; Bidlingmeier, B.; Stabel, A.; Rabe, J. P. *Angew. Chem., Int. Ed. Engl.* **1995**, *34*, 303−307.

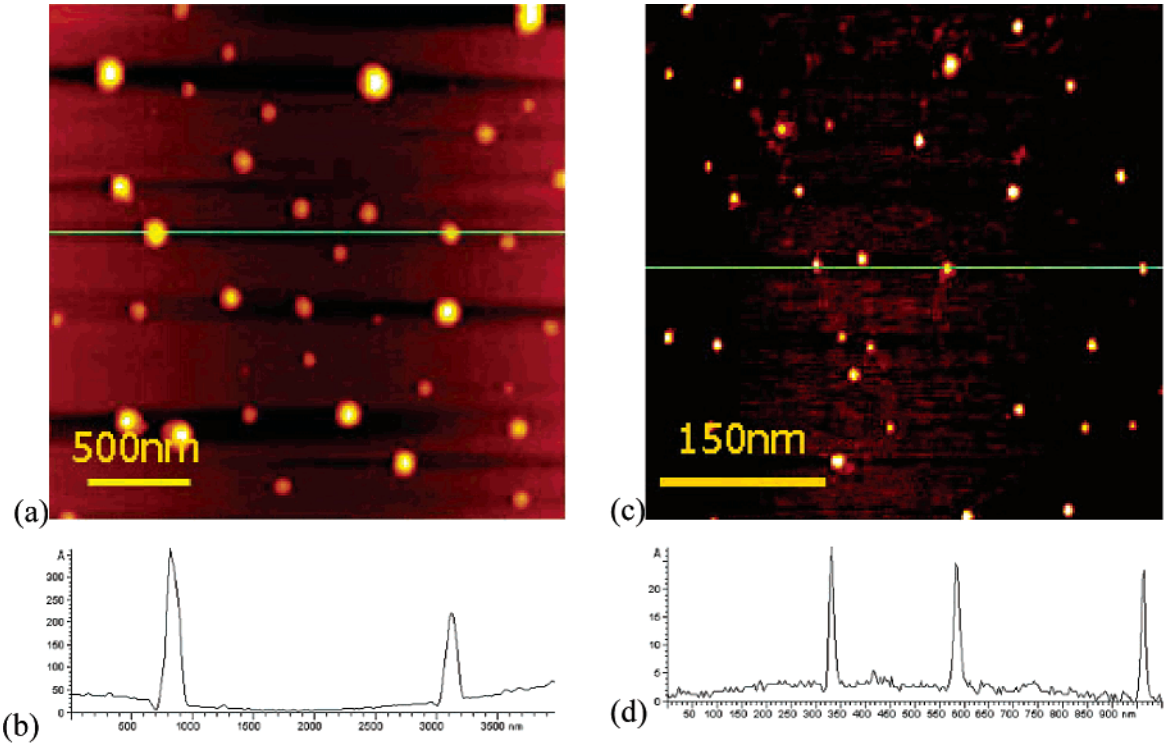

Figure 9. AFM topographic images and height profiles of the globular aggregates of **14T-1** and **30T** on mica. (a) AFM topographic image of the larger **14T-1** aggregates on mica; (b) height profile across the line in (a); (c) AFM topographic image of **30T** aggregates on mica; and (d) height profile across the line in (c).

container (solvent saturated). Figure 9a shows the AFM image of **14T-1** on mica from a 0.1 μM solution. Because of differences in the surface energy, the hydrophobic molecules tend to aggregate into globular objects on the hydrophilic surface of mica to minimize the surface energy. The sizes of these nanoparticle aggregates are not uniform, ranging from several nanometers to tens of nanometers. The aggregates formed on mica for **30T** are smaller and more uniform than that of **14T-1** (Figure 9c). The height of the aggregates is about 3 nm, which is in the single macromolecule range. However, it is not certain if they are dispersed singly because there is not enough information about the shape of the molecule in relation to their measured dimension. Liu et al. recently observed a very similar phenomenon from a polyphenylene dendrimer where globular aggregates with different sizes and single dendrimer molecules were imaged by AFM on mica.[10a] Thus, the difference in aggregation behavior of **14T-1** and **30T** is derived from different degrees of intermolecular interactions, which, in this case, is mainly due to the extent of $\pi-\pi$ interactions. The fact that **14T-1** formed larger aggregates shows that **14T-1** has stronger $\pi-\pi$ intermolecular interactions than does **30T**. It also indicates that **14T-1** adopts a more planar structure. This observation is also consistent with the MALDI-TOF-MS results, which showed strong aggregation peaks from **14T-1** in the form of n-mer derivatives.

When the dendrimers were cast on the HOPG surface at different concentrations, a remarkable difference was observed. By AFM observation, **14T-1** self-assembled into nanowire structures as shown in Figure 10. The length and diameter of the wires are not uniform and are very concentration dependent. Figure 10a displays the structure initially from a 0.11 μM solution. A lot of scattered dots (dendrimer aggregates) coexist on the surface besides for a few wires. The diameters of the wires are around 2−4 nm (based on height profile). This suggests that the wires are indeed one-molecule-wide columnar π-stacks. The role of the alkyl chains is also important because they can aid in stabilizing the columnar stacks while maintaining their solubility in the slowly evaporating solvent. When the concentration is further increased to 1.1 μM, the wire structures dominated the morphology of the adsorbed molecules without any globular aggregates, and the diameter of the wires varied. The large-diameter wires may be comprised of several bundles of individual thin wires. This remarkable nanowire formation again emphasizes the strong influence of the $\pi-\pi$ interactions between the **14T-1** molecules. Previous work by the Müllen group highlights the rationale for nanowire formation in conjugated polyphenylene dendrimers.[22]

In contrast to **14T-1**, **30T** formed 2-D crystals on the basal plane of a freshly cut HOPG substrate (lattice spacing of 0.246 nm) when cast from a dilute solution (0.58 μM). Figure 11 shows the STM image of the tight hexagonally packed dendrimer molecules. The unit cell dimensions are $a = b = 10 \pm 2$ nm, $\alpha = 62° \pm 2°$. The bright spots are attributed to the aromatic thiophene moieties. They appear brighter than the alkyl chains due to the smaller energy difference between their frontier orbitals and the Fermi level of the substrate. Note that it is not possible to resolve the alkyl chains due to their high conformational mobility at the time scale of STM imaging. Tunneling conditions for the STM image are as follows: $U_t = 0.1$ V, set point current = 1 nA. It is clear from the domain boundary and Moire patterns that the graphite surface is differentiated from the crystalline domain of the adsorbed dendrimers. Previous

(22) Liu, D.; Feyter, S. D.; Cotlet, M.; Wiesler, U.-M.; Weil, T.; Herrmann, A.; Mullen, K.; De Schryver, F. C. *Macromolecules* **2003**, *36*, 8489−8498.

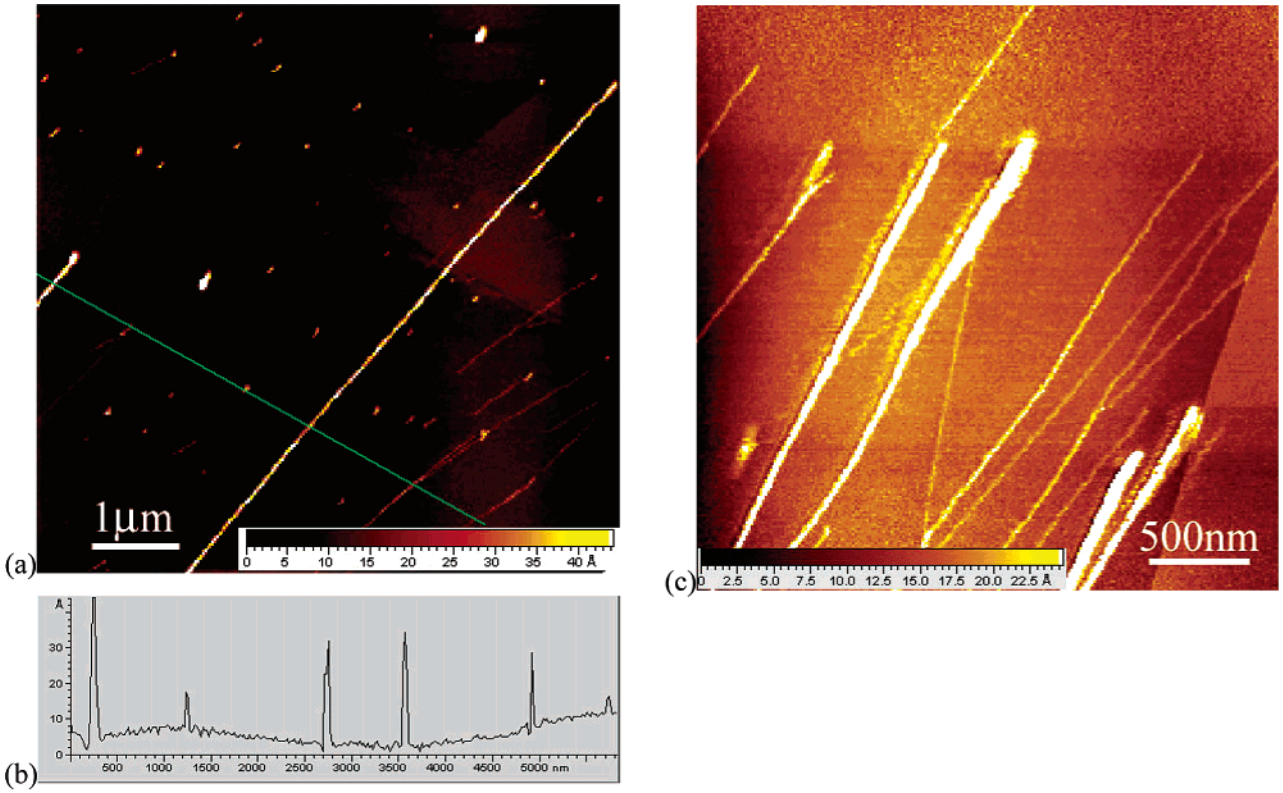

Figure 10. AFM topographic images of **14T-1**, showing the nanowire formation on graphite surface. The films were prepared from different concentration solutions: (a) 0.11 μM; (b) height profile across the line in (a); (c) 1.1 μM.

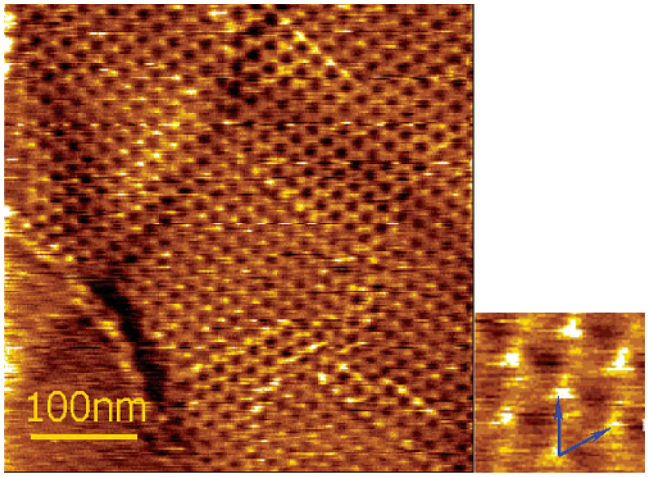

Figure 11. STM topographic image of the self-assembled hexagonal structure of **30T** on HOPG. The unit cell dimensions are $a = b = 10 \pm 2$ nm, $\alpha = 62° \pm 2°$. Tunneling conditions for the STM image: $U_t = 0.1$ V, set point current = 1 nA.

studies by Rabe et al.[23] showed that disklike dendrimer molecules can form crystalline monolayers on a graphite surface epitaxially at the liquid−solid interface due to the strong adsorption on the graphite surface. Dry monolayers with crystalline structures can also be observed by depositing from a very dilute solution. It was estimated that the adsorption energy in the gaseous environment of alkyl chains to graphite is about 7 kJ/mol,[24] while each phenylene subunit contributes about 15 kJ/mol[25] for the adsorption energy. The thiophene units in this system may not provide adsorption energy as strong as phenylene units; however, it should have significant contribution to the physisorption due to its aromaticity. Although a quantitative value has not been given, the physisorbed monolayers of linear and cyclic thiophene derivatives have also been demonstrated.[26] Again, the energy difference between the molecule−molecule and the molecule−substrate interactions plays an important role in determining the packing behavior. For **30T**, the molecule−substrate interactions dominate the packing of the molecules. The fact the **30T** formed 2-D crystals whereas the **14T-1** did not highlights the epitaxial nature of the deposition process. In this case, the lattice of the graphite substrate and it's contribution to the adsorption free energy is very good for the size of **30T** but not for the **14T-1**. The alkyl chain also greatly influences the packing arrangement through van der Waals interactions resulting in some interdigitation between alkyl chains of neighboring dendrimers. To confirm this rationale, we synthesized another **14T-1** molecule with a longer dodecyl side chain instead of a hexyl chain. The longer alkyl chain is expected to have a larger dimension than the hexyl derivative (in this case approximating **30T**). It should also have a higher molecule−substrate interaction that may overcome the stacking of the molecules into columns, thus also forming a 2-D crystalline structure on the graphite surface with a different lattice dimension. Indeed, Figure 12 shows an oblique 2-D packing and crystallization of this molecule on graphite. The unit cell dimensions are $a = 6.4 \pm 0.1$ nm, $b = 5.4 \pm 0.1$ nm,

(23) (a) Samori, P.; Severin, N.; Simpson, C. D.; Mullen, K.; Rabe, J. P. *J. Am. Chem. Soc.* **2002**, *124*, 9454−9457. (b) Samori, P.; Fechtenkotter, A.; Jackel, F.; Bohme, T.; Mullen, K.; Rabe, J. P. *J. Am. Chem. Soc.* **2001**, *123*, 11462−11467.

(24) Hentschke, R.; Schurmann, B. L.; Rabe, J. P. *J. Chem. Phys.* **1992**, *96*, 6213−6221.

(25) Vernov, A.; Steele, W. A. *Langmuir* **1991**, *7*, 3110−3117.

(26) Kromer, J.; Rios-Carreras, I.; Fuhrmann, G.; Musch, C.; Wunderlin, M.; Debaerdemarker, T.; Mena-Osteritz, E.; Bauerle, P. *Angew. Chem., Int. Ed.* **2000**, *39*, 3481−3486.

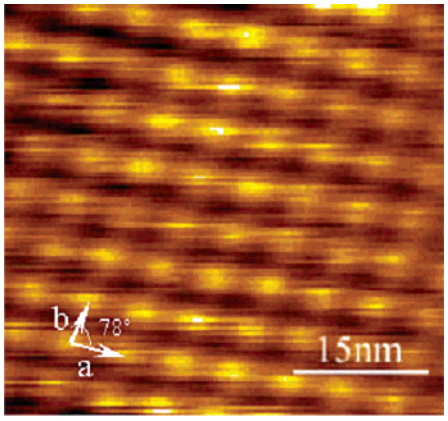

Figure 12. STM topographic image of the self-assembled structure of **14T** on HOPG. The unit cell dimensions are $a = 6.4 \pm 0.1$ nm, $b = 5.4 \pm 0.1$ nm, $\alpha = 78° \pm 2°$. Tunneling conditions for the STM image: $U_t = 0.1$ V, set point current = 1 nA.

$\alpha = 78° \pm 2°$. The tunneling conditions for the STM image are as follows: $U_t = 0.1$ V, set point current = 1 nA. Individual molecules can be clearly seen from the STM image. The different symmetry of the packing for **30T** and **14T-1** is dependent on several factors, such as the molecular shape, size, and the presence of noncovalent intermolecular interactions. Further STM imaging with other tunneling parameters can be done to refine the analysis of the packing behavior in these molecules. Nevertheless, these results highlight the unique ability of these dendrimers to form periodic nanostructures on highly ordered surfaces such as HOPG.

Conclusions

Dendritic thiophene derivatives have been designed and synthesized mainly by a convergent method. The structure and size of the dendrons and dendrimers have been confirmed with various techniques, such as NMR, SEC, and MALDI-TOF-MS. The ^{1}H NMR spectra showed interesting association behavior for **14T-1**, **14T-2**, and **30T** under different temperatures. MALDI-TOF mass values were consistent with the mass calculated from the expected structures. The SEC measurements gave useful information on the hydrodynamic volume of the individual dendrimers. However, the number-average molecular weights from SEC deviated from the true values, which is normal for rigid dendritic molecules when using polystyrene standards. These unsymmetrical dendrimers showed very broad absorption spectra, which could make them useful for light-harvesting molecules. The self-organization of the dendrimers on solid substrates is dependent on the nature of the substrates, preparation methods, and the molecule−molecule and molecule−substrate interactions. **14T-1** and **30T** both formed globular aggregates on mica surface. While **14T-1** also formed nanowires on graphite surface, **30T** formed 2-D crystalline structures. By varying the alkyl chain length attached to **14T-1**, we were able to obtain 2-D crystals for a dodecyl-substituted **14T-1** on graphite. These 2-D structures are of great interest for molecular electronics. The conformation of the molecules, that is, the torsion between the thiophene rings, is locked in the monolayer on the graphite surface. For example, by inducing a high voltage pulse through the STM tip to a single molecule, one may be able to change their conformation, thus changing the tunneling current and realizing ON/OFF states for these molecules. These experiments are currently under investigation.

Acknowledgment. We gratefully acknowledge partial funding from the Robert A. Welch Foundation (E-1551), NSF-CTS (0330127), and NSF-DMR (99-82010). We also thank Molecular Imaging for technical support.

Supporting Information Available: Experimental details include reference to the synthesis of the dendrimers, instrumentation for spectroscopy, microscopy, and electrochemistry. This includes electrochemical conditions and AFM and STM imaging procedures. This material is available free of charge via the Internet at http://pubs.acs.org.

JA0484404